HOKKAIDO UNIVERSITY

Title	Energy-Dissipative Matrices Enable Synergistic Toughening in Fiber Reinforced Soft Composites
Author(s)	Huang, Yiwan; King, Daniel R.; Sun, Tao Lin et al.
Citation	Advanced Functional Materials, 27(9), 1605350 https://doi.org/10.1002/adfm.201605350
Issue Date	2017-03-03
Doc URL	https://hdl.handle.net/2115/65142
Type	journal article
File Information	Supporting Information.pdf

Hokkaido University Collection of Scholarly and Academic Papers : HUSCAP

Copyright WILEY-VCH Verlag GmbH & Co. KGaA, 69469 Weinheim, Germany, 2017.

ADVANCED FUNCTIONAL MATERIALS

Supporting Information

for *Adv. Funct. Mater.*, DOI: 10.1002/adfm.201605350

Energy-Dissipative Matrices Enable Synergistic Toughening in Fiber Reinforced Soft Composites

*Yiwan Huang, Daniel R. King, Tao Lin Sun, Takayuki Nonoyama, Takayuki Kurokawa, Tasuku Nakajima, and Jian Ping Gong**

Copyright WILEY-VCH Verlag GmbH & Co. KGaA, 69469 Weinheim, Germany, 2016.

Supporting Information

Energy-Dissipative Matrices Enable Synergistic Toughening in Fabric Reinforced Soft Composites

*Yiwan Huang, Daniel R. King, Tao Lin Sun, Takayuki Nonoyama, Takayuki Kurokawa, Tasuku Nakajima, and Jian Ping Gong**

Table of contents:

Figure S1 (Page 2)

Table S1 (Page 2−3)

Figure S2−17 (Page 4−17)

Table 2 (Page 18)

Figure S18−20 (Page 19−21)

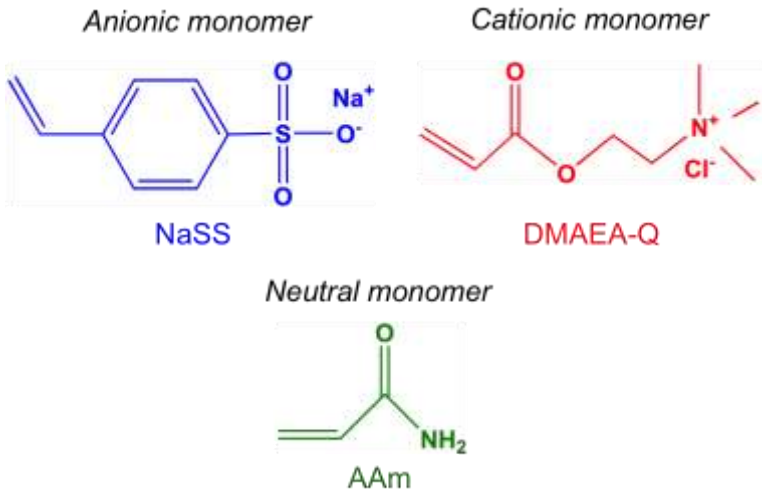

Figure S1. Chemical structures of the monomers used in this work. NaSS: sodium *p*-styrenesulfonate, DMAEA-Q: dimethylaminoethylacrylate quaternized ammonium, AAm: acrylamide.

Table S1. Weight fraction and volume fraction of each component in neat PA hydrogel and PA-GF hydrogel composites.

Name of sample	Weight fraction, W (wt%)			Volume fraction, Φ (vol%)		
	W_{fiber}	$W_{polymer}$	W_{water}	Φ_{fiber}	$\Phi_{polymer}$	Φ_{water}
As-prep. PA	0.00	44.35 ± 0.86	55.65 ± 0.86	0.00	34.17 ± 3.70	65.83 ± 3.70
Equil. PA	0.00	52.16 ± 0.90	47.84 ± 0.90	0.00	53.72 ± 5.81	46.28 ± 5.81
As-prep. PA-GF	29.88 ± 0.18	31.10 ± 0.08	39.02 ± 0.10	13.65 ± 0.05	31.77 ± 0.03	54.58 ± 0.02
Equil. PA-GF	33.38 ± 0.19	34.75 ± 0.11	31.87 ± 0.09	18.75 ± 0.07	43.65 ± 0.04	37.60 ± 0.03

The weight fraction of water (W_{water}, wt%) in the hydrogel samples was measured with a moisture balance (MOC-120H, SHIMADZU Co., Japan) based on the equation $W_{water} = \frac{m_{water}}{m_{sample}} * 100\%$, where m_{water} (g) is the weight of water in the hydrogel network, and m_{sample} (g) is the weight of the whole hydrogel sample. The weight fraction of glass fiber (W_{fiber}, wt%) in the hydrogel composite samples was calculated by the equation $W_{fiber} = \frac{\sigma_s * A}{m_{composite}} *$

100%, where σ_s (= 590 g m^{-2}), A (m^2), and $m_{composite}$ (g) are the surface density of glass fiber fabric, the surface area of the fabric, and the weight of the hydrogel composite sample, respectively. The weight fraction of polymer ($W_{polymer}$, wt %) for both the neat hydrogels and hydrogel composites was calculated by the equations $W_{\mathrm{polymer}} = (100\% - W_{\mathrm{water}})$ and $W_{\mathrm{polymer}}' = (100\% - W_{\mathrm{water}} - W_{\mathrm{fiber}})$, respectively.

The volume fraction of water (Φ_{water}, vol%) in the hydrogel samples was calculated by the equation $\Phi_{\mathrm{water}} = \frac{W_{\mathrm{water}} \cdot m_{\mathrm{sample}}}{\rho_{\mathrm{water}} \cdot V_{\mathrm{sample}}} * 100\%$, where ρ_{water} (≈ 0.998 g cm^{-3}) is the density of water, and V_{sample} is the volume of the whole hydrogel sample. The volume fraction of fiber (Φ_{fiber}, vol%) in the hydrogel composite samples was determined by the equation $\Phi_{\mathrm{fiber}} = \frac{\sigma_s * A}{\rho_{\mathrm{E-glass}} \cdot V_{\mathrm{sample}}} * 100\%$, where $\rho_{E\text{-}glass}$ (≈ 2.55 g cm^{-3}) is the density of E-glass used to fabricate the fiber fabric in this work. The volume fraction of polymer ($\Phi_{polymer}$, vol%) for both the neat hydrogels and hydrogel composites was calculated by the equations $\Phi_{\mathrm{polymer}} = (100\% - \Phi_{\mathrm{water}})$ and $\Phi_{\mathrm{polymer}}' = (100\% - \Phi_{\mathrm{water}} - \Phi_{\mathrm{fiber}})$, respectively.

At least three tests were carried out for each sample, and the average value was calculated and the standard derivation was obtained as the error bar.

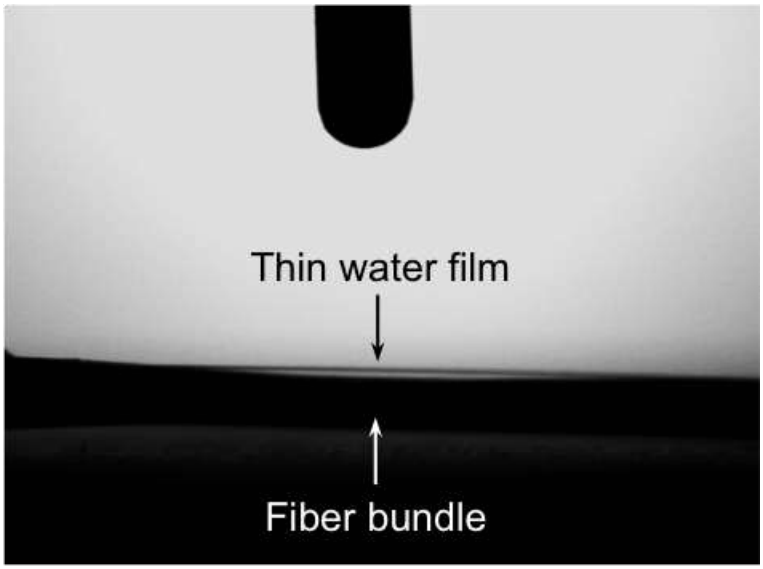

Figure S2. Photograph of a contact angle test in air. When a water droplet is placed on a glass fiber bundle, it immediately wets the hydrophilic glass fibers[1–4] and penetrates into the fiber bundle due to the capillary effect (indicated by the thin water film). Owing to this feature, the precursor solution of PA hydrogel can excellently penetrate into the fiber bundle to form a composite with good interfacial contact.

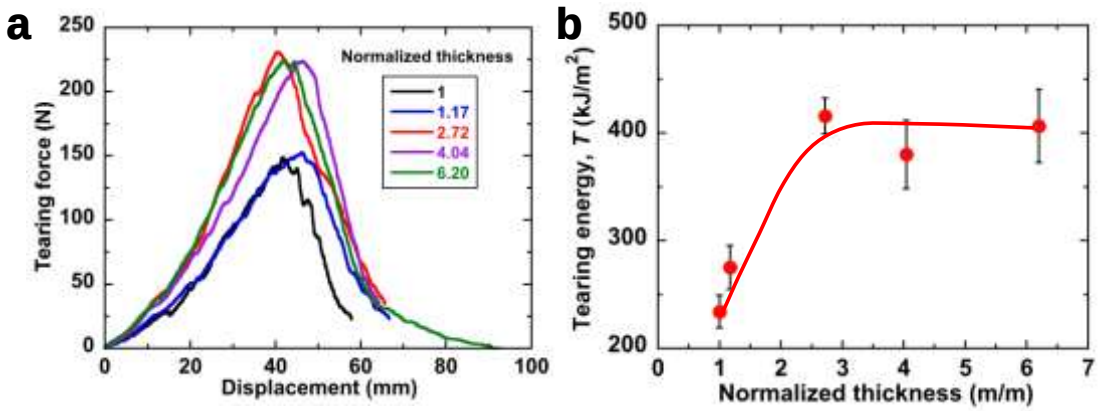

Figure S3. Tearing behavior of PA-GF hydrogel composites with different sample thicknesses. (a) The raw tearing force *vs.* displacement curves for the composites with different thicknesses. (b) The tearing energy *vs.* the normalized thickness. The sample width of all the composites is w = 45 mm, and the tearing velocity is 50 mm min^{-1}. The thickness of hydrogel composites was tuned by changing the thickness of the silicone spacer. The normalized thickness represents the thickness of the as-prepared hydrogel composite divided by the thickness of GF (t = ~0.59 mm). The critical thickness in our PA hydrogel composites appears to be ~3 times fabric thickness (~1.50 mm), which is smaller than the dissipation zone measured for neat PA gels (~5 mm).[5] The difference is probably due to the relatively small deformation in the z-axis (out of plane) direction due to the two-dimensional (x- and y-axes) plain structure of the fabric.

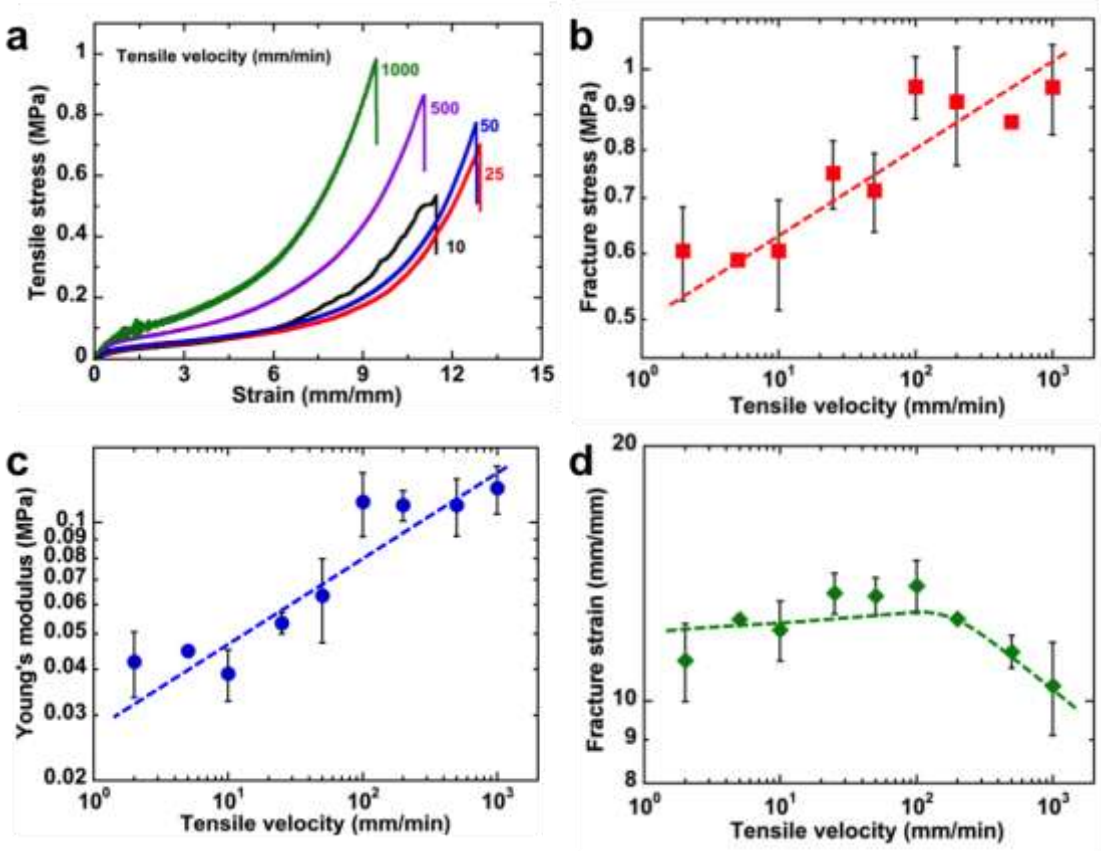

Figure S4. Tensile velocity dependent behaviors of neat H_2O-equilibrated polyampholyte (PA) hydrogels. (a) Stress-strain curves; (b) Fracture stress; (c) Young's modulus; (d) Fracture strain. The initial gauge length of dumbbell-shaped sample is 12 mm. Dashed lines in (b), (c), and (d) are manually drawn as visual guides.

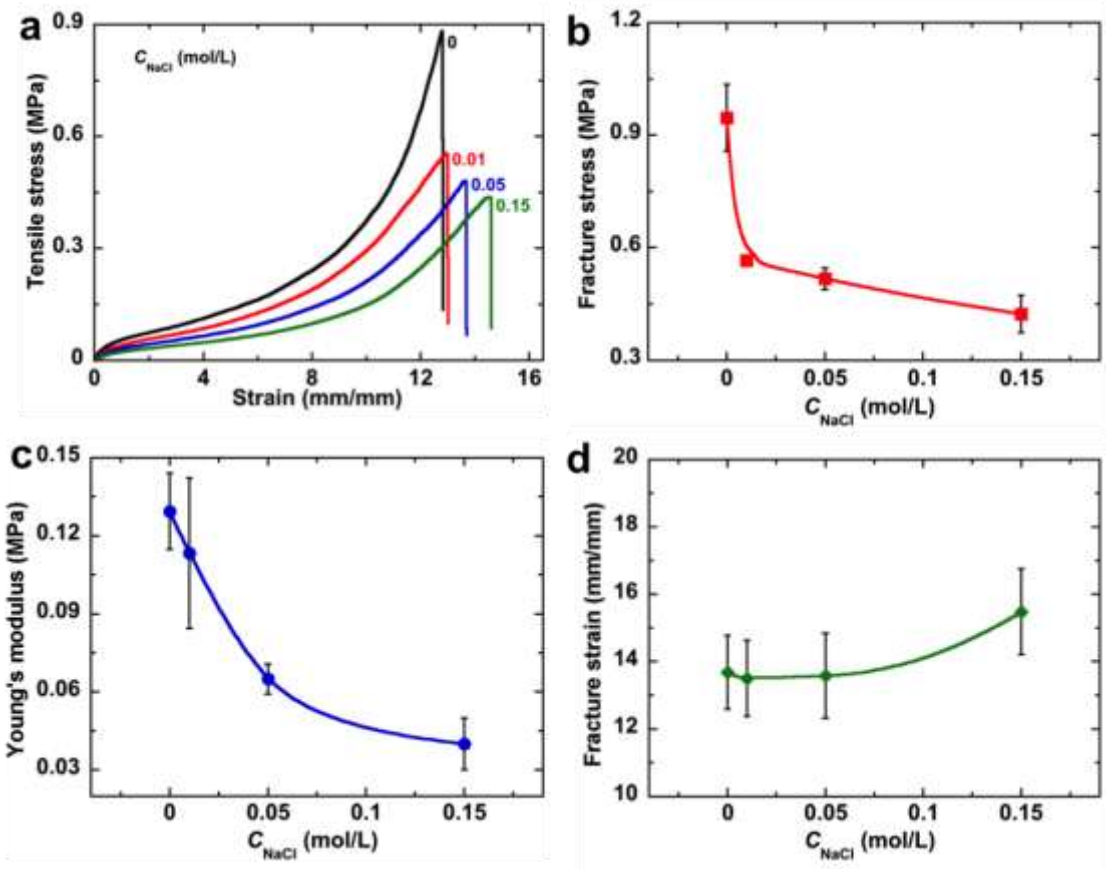

Figure S5. Tensile behavior of neat PA hydrogels after achieving the equilibrium in NaCl solutions with different salt concentrations. (a) Stress-strain curves; (b) Fracture stress; (c) Young's modulus; (d) Fracture strain.

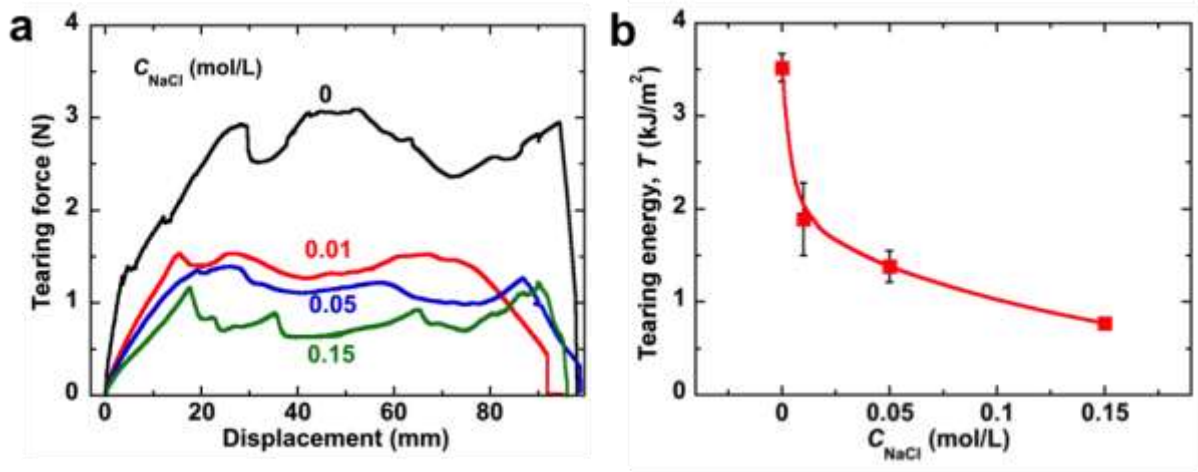

Figure S6. Tearing behavior of neat PA hydrogels after achieving the equilibrium in NaCl solutions with different salt concentrations. (a) Tearing force *vs.* displacement curves; (b) Tearing energy, *T*, *vs.* salt concentration, C_{NaCl}. The tearing velocity is 50 mm min^{-1}.

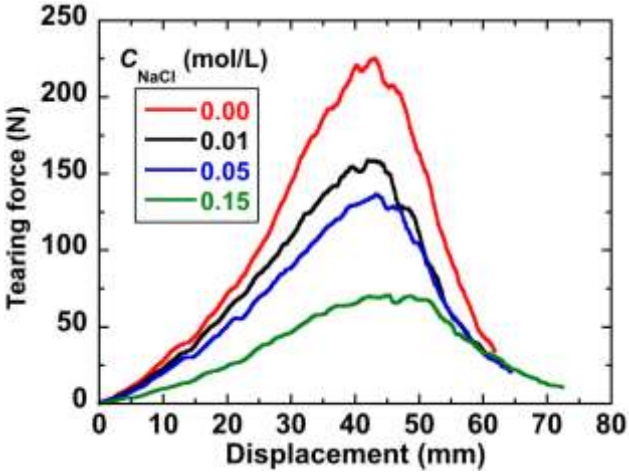

Figure S7. Tearing force *vs.* displacement curves of PA-GF hydrogel composites after the equilibrium in NaCl solutions with different salt concentrations. The tearing velocity is 50 mm min^{-1}.

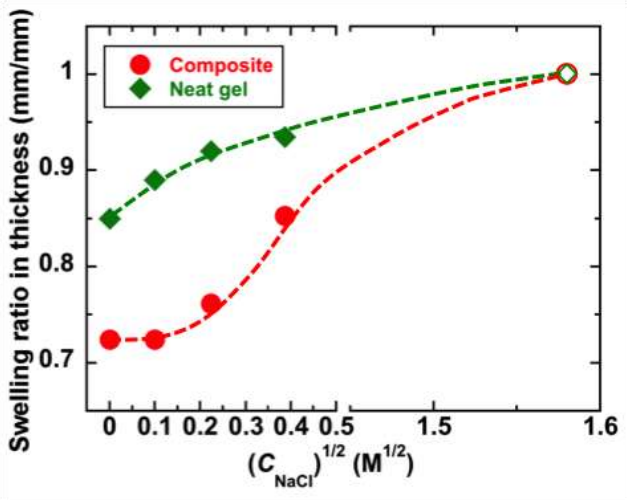

Figure S8. Swelling ratio (in thickness direction) *vs.* $C_{NaCl}^{1/2}$, for the PA hydrogel and the PA-GF gel composites. Here the swelling ratio is normalized by the thickness of their as-prepared samples. The open symbols represent the results of the as-prepared samples (salt concentration: 2.5 M). Dashed lines are manually drawn as visual guides.

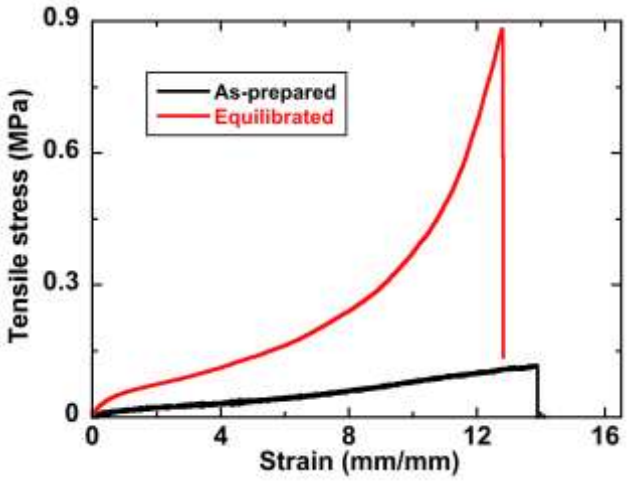

Figure S9. Tensile behaviors of as-prepared and H_2O-equilibrated polyampholyte hydrogels. The tensile velocity is 100 mm min^{-1}. The detailed mechanical properties: (1) as-prepared PA gel: Young's modulus, E = 0.02 ± 0.005 MPa, fracture stress, σ = 0.14 ± 0.029 MPa, and fracture strain, ε = 12.30 ± 1.38 mm mm^{-1}; (2) equilibrated PA gel: E = 0.13 ± 0.015 MPa, σ = 0.95 ± 0.089 MPa, and ε = 13.68 ± 1.09 mm mm^{-1}. The equivalent salt

concentration in the as-prepared PA gels is 2.5 M. This result is in consistent with the results of samples in saline solution.

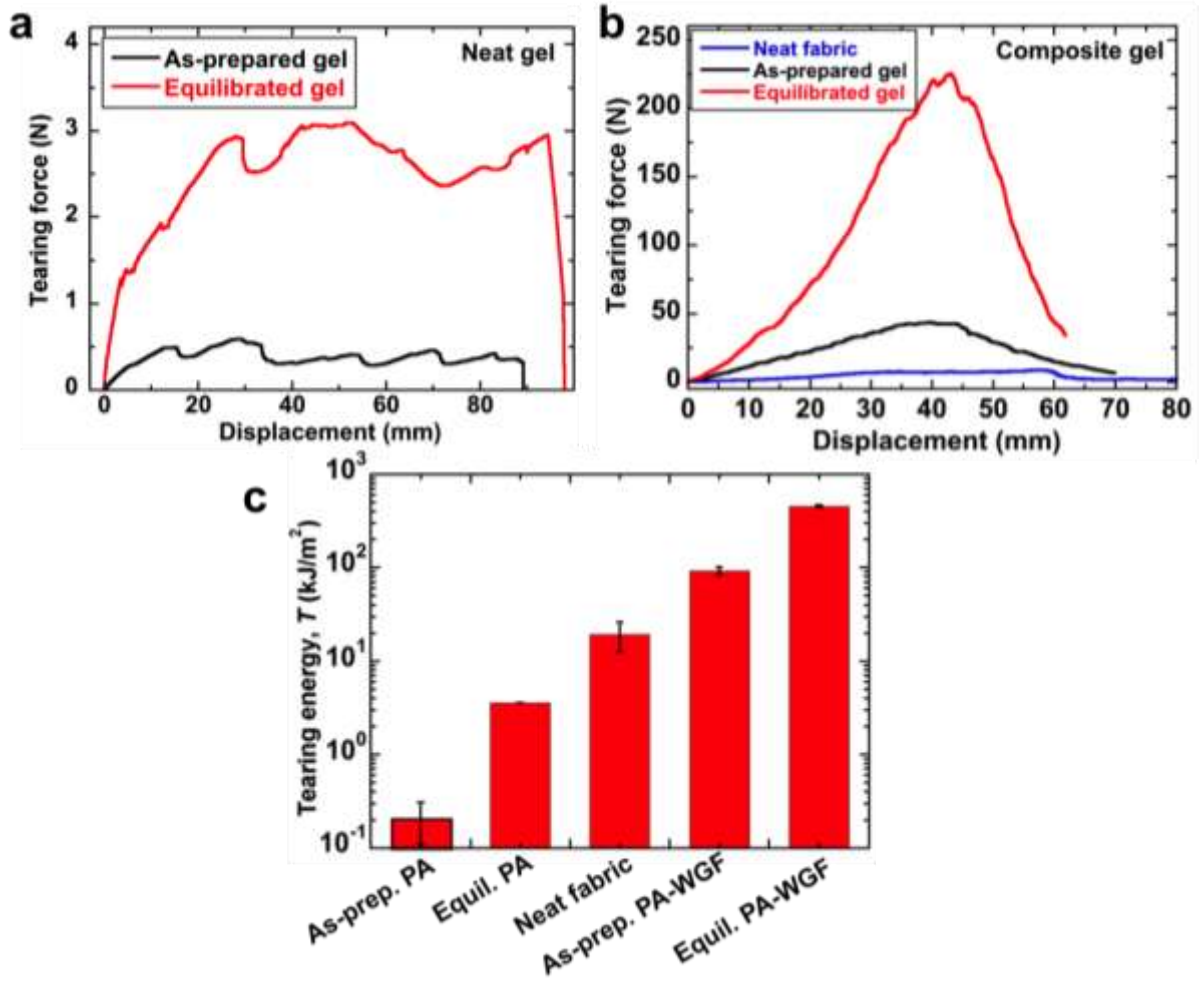

Figure S10. Tearing behaviors of the as-prepared and H_2O-equilibrated PA hydrogels and their corresponding PA-GF hydrogel composites. The tearing velocity is 50 mm min^{-1}. (a) Tearing force *vs.* displacement curves for the as-prepared and equilibrated neat PA gels. The thicknesses of as-prepared and equilibrated samples are ~2.00 mm and ~1.73 mm, respectively. (b) Tearing force *vs.* displacement curves for the as-prepared and equilibrated PA-GF gel composites, with w = 45 mm. (c) Tearing energy, T, of the above samples. The result of neat fabric is also shown.

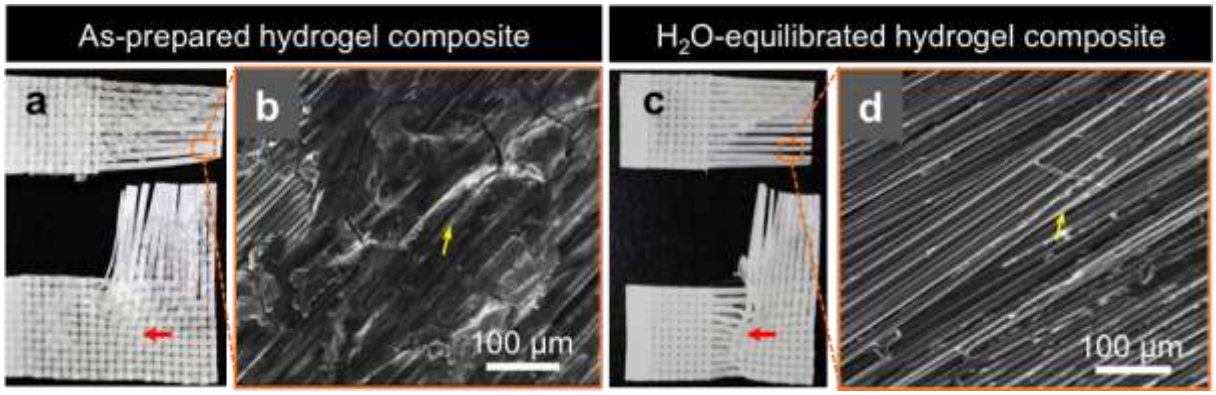

Figure S11. Macro- and micrographs of the as-prepared and H_2O-equilibrated PA-GF hydrogel composites after fracture. The red arrow in each macrograph indicates the area where residual deformation is seen. Comparing with the equilibrated sample, the as-prepared sample shows negligible residual deformation. The yellow arrow indicates the hydrogel matrix adhered on the fibers after the tearing test.

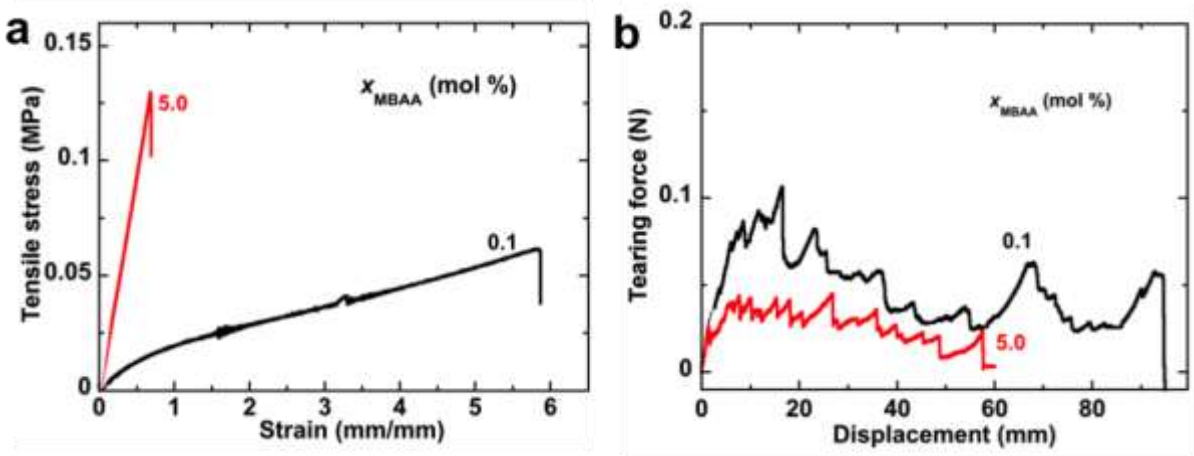

Figure S12. Tensile and tearing behaviors of as-prepared neat polyacrylamide (PAAm) hydrogels with different crosslinker (MBAA) fractions (x_{MBAA}) in relation to the total monomer concentration. (a) Stress-strain curves. The tensile velocity is 100 mm min^{-1}. (b) Tearing force *vs.* displacement curves. The tearing velocity is 50 mm min^{-1}. The detailed mechanical properties: (1) PAAm gel-0.10% MBAA: Young's modulus, E = 0.03 ± 0.000 MPa, fracture stress, σ = 0.08 ± 0.021 MPa, fracture strain, ε = 7.33 ± 2.12 mm mm^{-1}, and tearing energy, T = 0.06 ± 0.01 kJ m^{-2}; (2) PAAm gel-5.0% MBAA: E = 0.19 ± 0.01 MPa, σ = 0.10 ± 0.024 MPa, ε = 0.49 ± 0.13 mm mm^{-1}, and T = 0.034 ± 0.007 kJ m^{-2}.

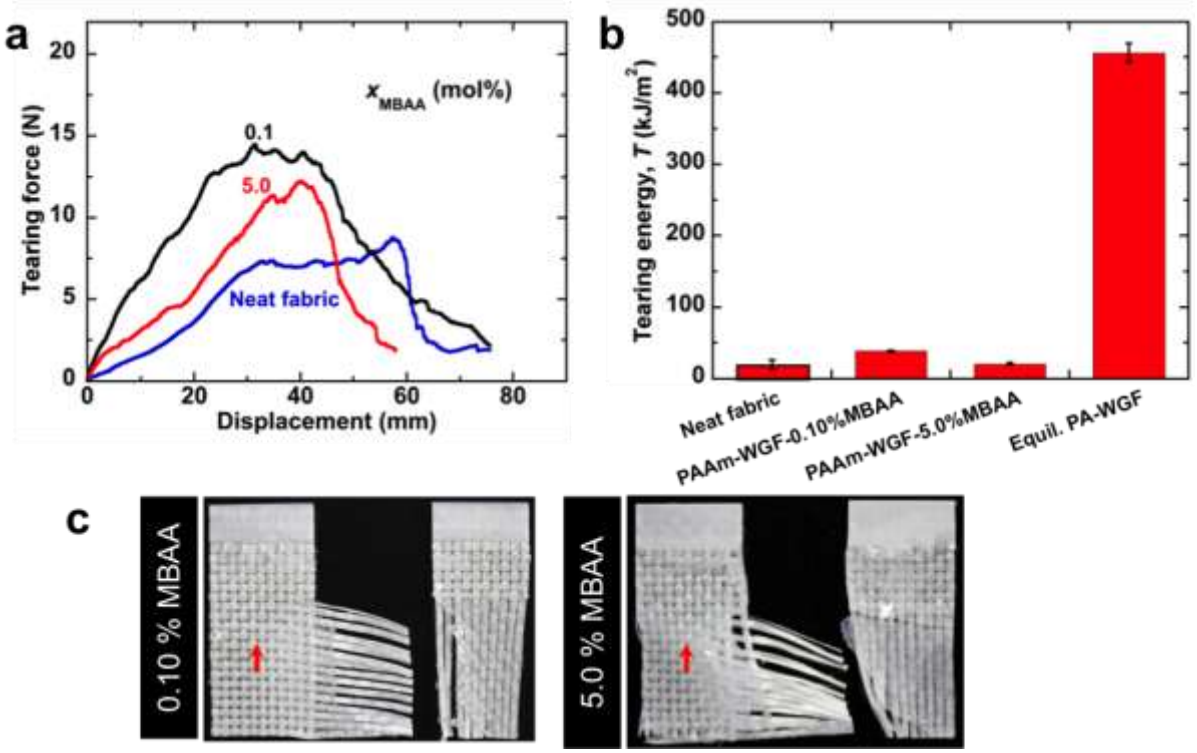

Figure S13. Tearing behavior of as-prepared PAAm-GF hydrogel composites with different crosslinker (MBAA) fractions (x_{MBAA}) in relation to the total monomer concentration. (a) Tearing force *vs.* displacement curves for the hydrogel composites and neat fabric. The tearing velocity is 50 mm min^{-1}. (b) Tearing energy, *T*, of the above two groups and neat fabric as well as H_2O-equilibrated PA-GF hydrogel composite. The width of all the samples for the tearing test is w = 45 mm. (c) Fracture images of the composite hydrogels. The red arrow in each graph indicates the area where residual deformation is seen. Both of the two samples show no sign of residual deformation.

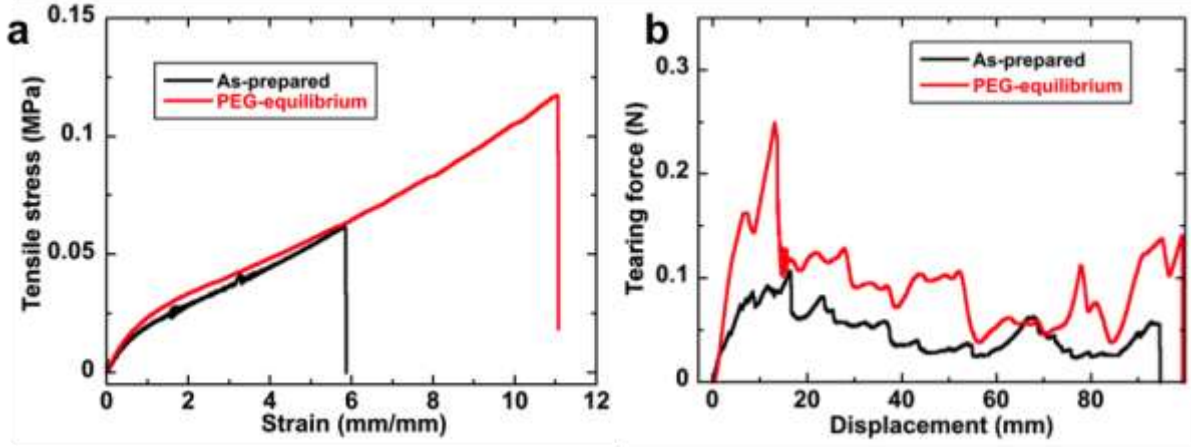

Figure S14. Tensile and tearing behaviors of as-prepared neat PAAm hydrogel and the PAAm hydrogel equilibrated in 20 wt% PEG solution. (a) Tensile stress *vs.* strain curves. The tensile velocity is 100 mm min^{-1}. (b) Tearing force *vs.* displacement curves. The tearing velocity is 50 mm min^{-1}. The crosslinker molar fraction of the as-prepared PAAm hydrogel is 0.10 mol %. The volume-swelling ratio of the PEG-deswollen PAAm gel is ~0.70 mm^3 mm^{-3} in relation to the as-prepared state, close to that of neat PA gel (monomer concentration: 2.5 M). The detailed mechanical properties: (1) as-prepared PAAm gel: Young's modulus, E = 0.03 ± 0.000 MPa, fracture stress, σ = 0.08 ± 0.021 MPa, fracture strain, ε = 7.33 ± 2.12 mm mm^{-1}, and tearing energy, T = 0.06 ± 0.01 kJ m^{-2}; (2) PEG-equilibrated PAAm gel: E = 0.035 ± 0.007 MPa, σ = 0.13 ± 0.007 MPa, ε = 12.05 ± 1.38 mm mm^{-1}, and T = 0.09 ± 0.01 kJ m^{-2}.

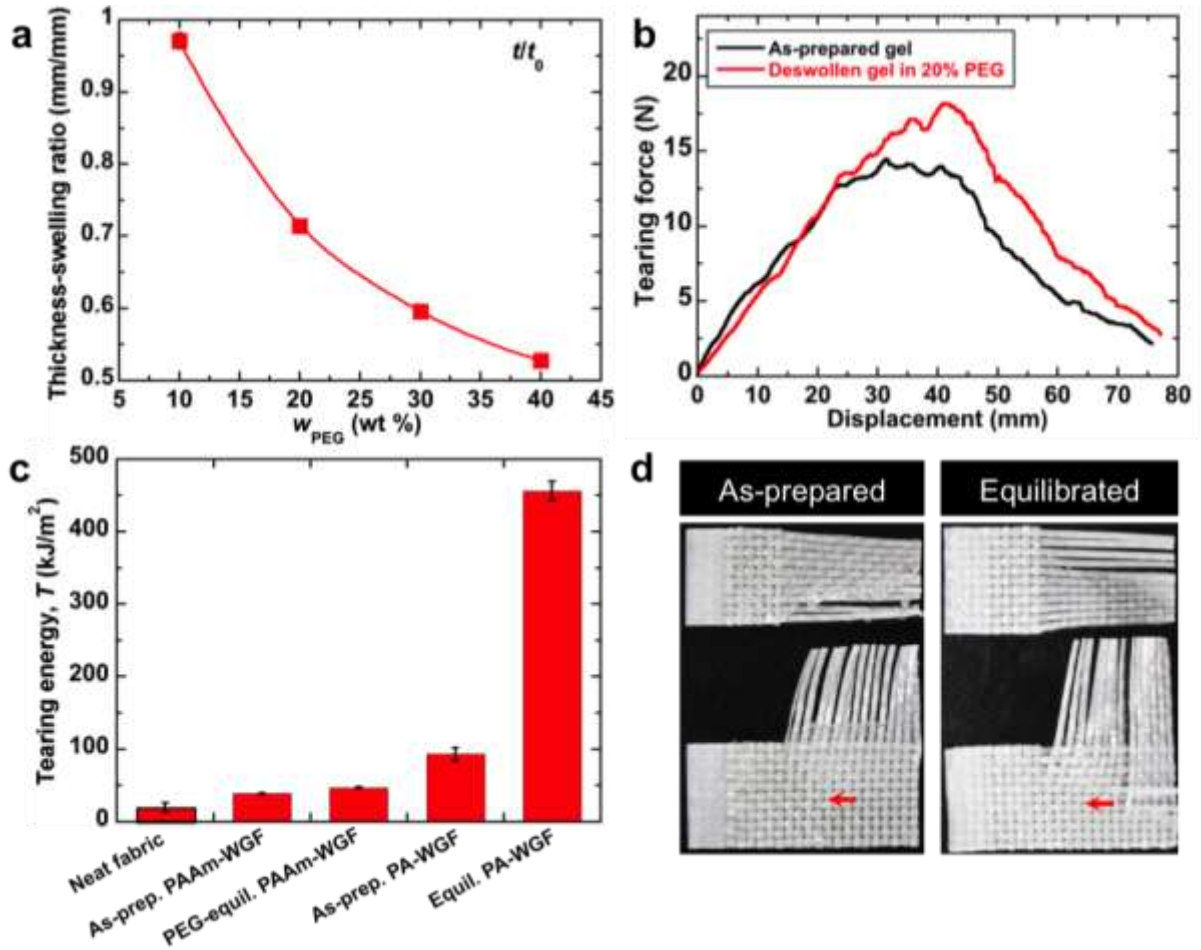

Figure S15. Tearing behavior of deswollen PAAm-GF hydrogel composite in concentrated poly(ethylene glycol) (M_w = 20,000) solutions. (a) Swelling ratio (in thickness direction) of the composite hydrogel in PEG solutions with different concentrations. (b) Tearing force *vs.* displacement curves for the as-prepared hydrogel composite and deswollen hydrogel composite in 20 wt% PEG solution, with w = 45 mm. Here 20 wt% PEG solution was used to deswell the PAAm-GF hydrogel composite for achieving the similar deswelling ratio (in thickness direction) as that of PA-GF hydrogel composite. The tearing velocity is 50 mm min^{-1}. (c) Tearing energy, T, of the above two groups and as-prepared as well as H_2O-equilibrated PA-GF hydrogel composites. (d) Fracture images of the composite hydrogel samples based on the above two groups. The red arrow in each graph indicates the area where residual deformation is seen. Both of the two samples show no sign of residual deformation.

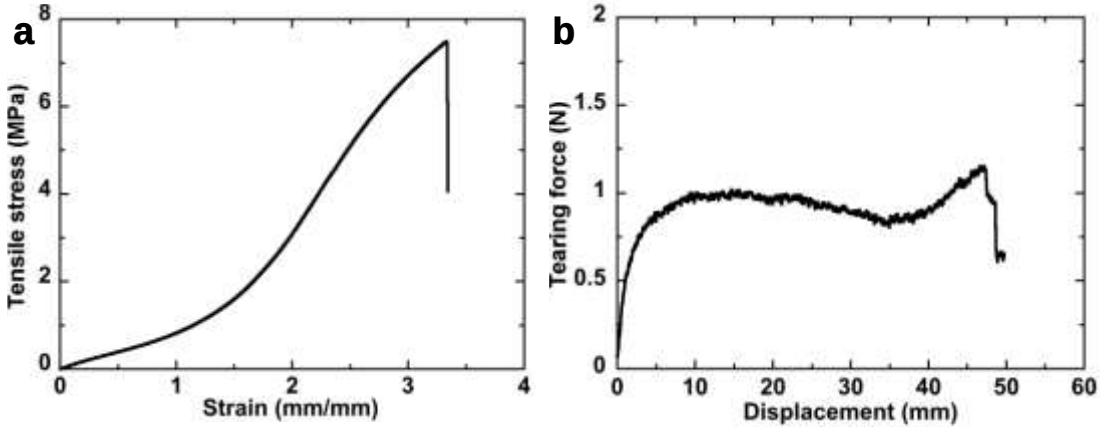

Figure S16. Tensile behavior and tearing behavior of neat PDMS elastomer. (a) Tensile stress *vs.* strain curve. The tensile velocity is 100 mm min^{-1}. (b) Tearing force *vs.* displacement curve. The tearing velocity is 50 mm min^{-1}. The sample thickness for the tearing test is ~1.98 mm. The detailed mechanical properties of PDMS elastomer: Young's modulus, E = 0.88 ± 0.03 MPa, fracture stress, σ = 6.75 ± 1.05 MPa, fracture strain, ε = 2.97 ± 0.53 mm mm^{-1}, and tearing energy, T = 0.96 ± 0.08 kJ m^{-2}.

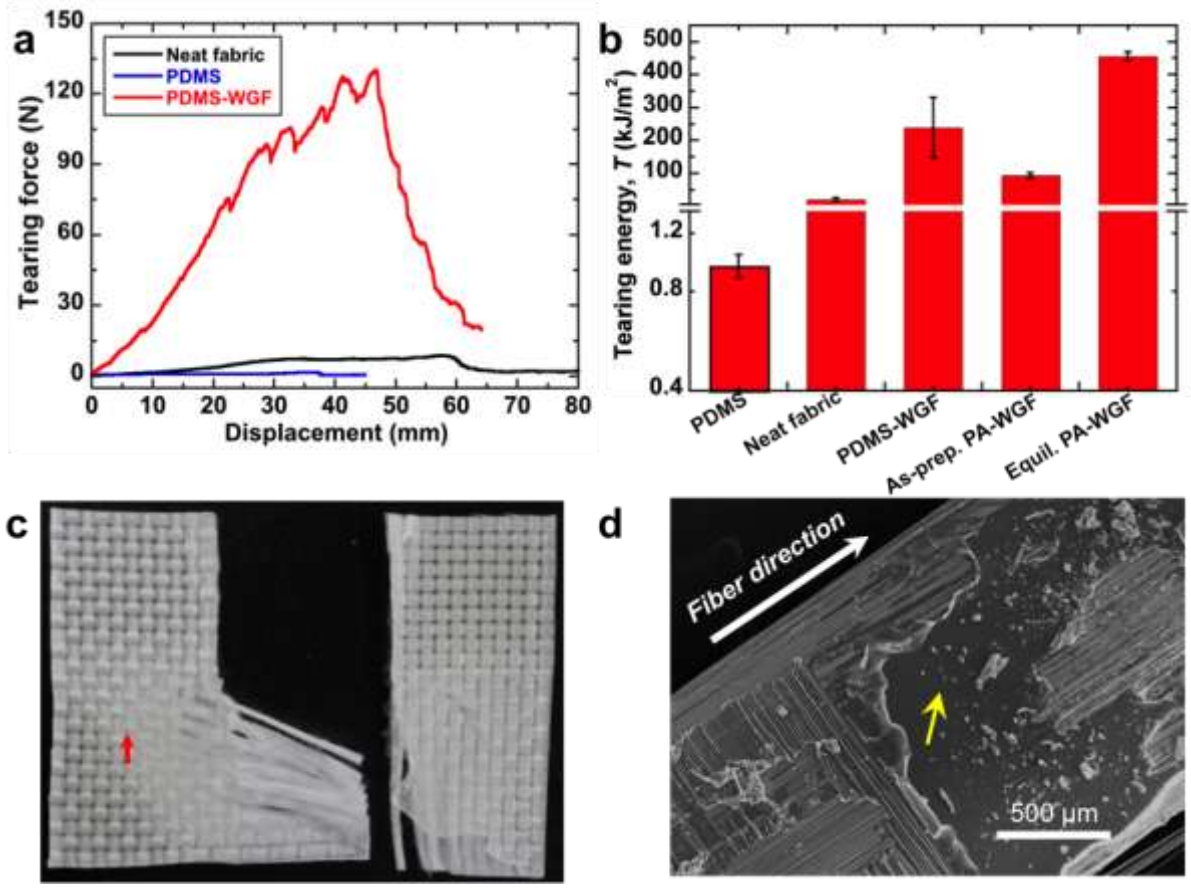

Figure S17. Tearing behavior of the PDMS-GF composite. (a) Tearing force *vs.* displacement curves for the neat fabric, PDMS elastomer, and PDMS-GF composite, with sample width w = 45 mm. The tearing velocity is 50 mm min^{-1}. The thicknesses of the three groups are ~0.59, ~1.98, and ~2.00 mm, respectively. (b) Tearing energy, T, comparison of the neat fabric, PDMS elastomer, PDMS-GF composite, and as-prepared and H_2O-equilibrated PA-GF hydrogel composites. (c) Fracture image of the PDMS-GF composite. The red arrow in the macrograph indicates the area where residual deformation is seen. The composite sample shows negligible residual deformation. (d) SEM image of the PDMS-GF composite.

Table S2. Mechanical properties of neat soft matrices and their GF composites (Sample width, w = 45 mm).

Name of soft matrix	Modulus E_n [MPa]	Fracture stress σ_n [MPa]	Fracture strain ε_n [mm mm^{-1}]	Tearing energy of neat matrix T_{matrix} [kJ m^{-2}]	Tearing energy of composite $T_{composite}$ [kJ m^{-2}]
As-prepared PA gel[1)]	0.02 ± 0.005	0.14 ± 0.029	12.30 ± 1.38	0.21 ± 0.10	92.98 ± 9.02
H_2O-equilibrated PA gel[1)]	0.13 ± 0.015	0.95 ± 0.089	13.68 ± 1.09	3.51 ± 0.15	456.04 ± 13.11
PA gel-0.01 M NaCl[1)]	0.11 ± 0.029	0.57 ± 0.006	13.50 ± 1.13	1.89 ± 0.39	311.30 ± 17.94
PA gel-0.05 M NaCl[1)]	0.07 ± 0.006	0.52 ± 0.029	13.58 ± 1.26	1.38 ± 0.17	254.12 ± 8.58
PA gel-0.15 M NaCl[1)]	0.04 ± 0.01	0.42 ± 0.050	15.48 ± 1.27	0.77 ± 0.03	159.37 ± 1.21
PA gel-2 mm min^{-1} [2)]	0.042 ± 0.008	0.605 ± 0.078	11.16 ± 1.17	0.752 ± 0.171	214.34 ± 0.00
PA gel-10 mm min^{-1} [2)]	0.039 ± 0.006	0.605 ± 0.092	12.14 ± 0.98	1.45 ± 0.28	345.54 ± 0.00
PA gel-100 mm min^{-1} [2)]	0.11 ± 0.022	0.95 ± 0.08	13.66 ± 0.98	3.10 ± 0.54	542.74 ± 0.00
PA gel-500 mm min^{-1} [2)]	0.11 ± 0.020	0.87 ± 0.007	11.44 ± 0.50	4.51 ± 0.90	492.88 ± 25.63
PA gel-1000 mm min^{-1} [2)]	0.12 ± 0.018	0.95 ± 0.12	10.42 ± 1.31	4.96 ± 0.66	500.56 ± 28.42
As-prepared PAAm gel-0.10 % MBAA [1)]	0.03 ± 0.000	0.08 ± 0.021	7.33 ± 2.12	0.06 ± 0.01	38.50 ± 1.20
As-prepared PAAm gel-5.0 % MBAA [1)]	0.19 ± 0.01	0.10 ± 0.024	0.49 ± 0.13	0.034 ± 0.007	20.56 ± 1.61
20 wt% PEG-deswollen PAAm gel [1)]	0.04 ± 0.007	0.13 ± 0.007	12.05 ± 1.38	0.09 ± 0.01	46.94 ± 1.04
PDMS elastomer [1)]	0.88 ± 0.03	6.75 ± 1.05	2.97 ± 0.53	0.96 ± 0.08	238.65 ± 92.34

1) Tensile velocity: 100 mm min^{-1}; tearing velocity: 50 mm min^{-1}.
2) Equilibrated in water.

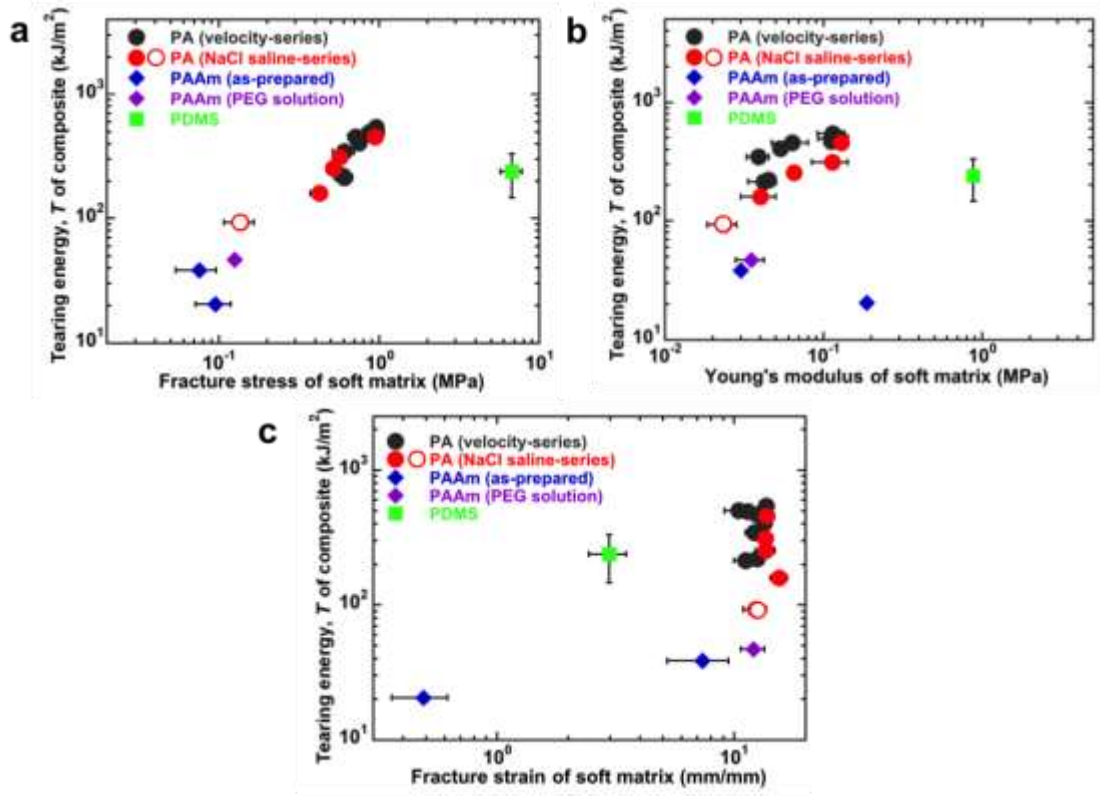

Figure S18. Tearing energy of the soft matrix-GF composite materials, $T_{\text{composite}}$, as a function of other mechanical properties based on different soft matrices. (a) $T_{\text{composite}}$ *vs.* fracture stress of soft matrices. (b) $T_{\text{composite}}$ *vs.* tensile modulus of soft matrices. (c) $T_{\text{composite}}$ *vs.* fracture strain of soft matrices. In these plots, two series of polyampholyte (PA) tough hydrogels at different conditions, polyacrylamide (PAAm) weak hydrogels at different conditions, and a commercially available polydimethylsiloxane (PDMS) elastomer are utilized as soft matrices in the composites. In detail, in one series utilizing the PA hydrogel matrix (black circles, "PA (velocity series)"), the hydrogel toughness was tuned by changing the tearing velocity ranging from 1 to 1000 mm min^{-1}, based on the strong viscoelasticity of PA gels. In the other series of the PA hydrogel matrix (red circles, "PA (NaCl saline series)"), the hydrogel toughness was tuned using saline solutions with different salt concentrations (0 ~ 0.15 M), because the ionic complex in PA gel network is sensitive

to external salt ions. The open red circle represents the result of as-prepared sample (salt concentration: 2.5 M). In one PAAm weak hydrogel matrix series (blue diamonds, "PAAm (as-prepared)"), the modulus and strength of the hydrogel were tuned by adjusting the chemical crosslinker percentage, yet the hydrogel toughness showed a slight change (see details in Figure S12 and S13). Meanwhile, the as-prepared PAAm hydrogel was also deswollen in 20 wt% poly(ethylene glycol) (PEG, M_w = 20,000) solution (purple diamond, "PAAm (PEG solution)") to achieve a similar deswelling behavior as the as-prepared PA hydrogel shows in deionized water, leading to slightly enhanced mechanical properties and toughness (see details in Figure S14 and S15). A PDMS elastomer (green squares, "PDMS") with a moderate tearing energy (~960 J m^{-2}) was also selected as a matrix (see details in Figure S16 and S17). The width of all composite samples for the tearing test is w = 45 mm.

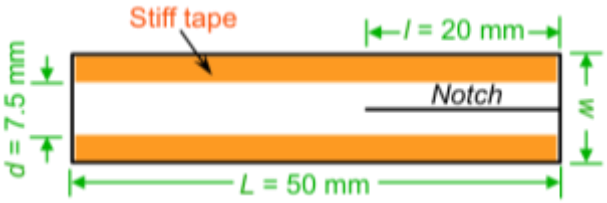

Figure S19. Geometry of the tearing test sample. For the neat hydrogel samples, to prevent the elongation of the legs of sample during the test, stiff and thin tapes (indicated by orange color) were glued on the both sides of samples prior to the test. The dimension of the *neat hydrogel samples*: full length L = 50 mm, initial notch length l = ~20 mm, width w = ~15 mm, effective distance d = ~7.5 mm, and thickness t = 1~2 mm. The dimension of the *hydrogel composite samples*: full length L = 50 mm, initial notch length l = ~20 mm, width w = 45 mm, and thickness t = 1 ~ 2 mm.

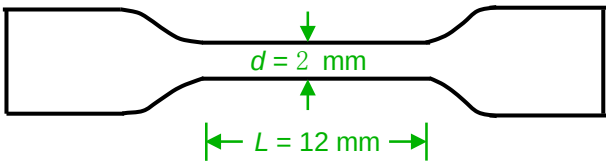

Figure S20. Geometry of the dumbbell-shaped sample for the tensile test. The *neat hydrogel* samples were cut into a dumbbell shape standardized as JIS-K6251-7 (2 mm in inner width, 12 mm in gauge length, and 1 ~ 2 mm in sample thickness) with a gel-cutting machine (Dumb Bell Co., Ltd.).

Supplementary References

[1] V. Gun'ko, V. Zarko, V. Turov, R. Leboda, E. Chibowski, E. Pakhlov, E. Goncharuk, M. Marciniak, E. Voronin, A. Chuiko, *J. Colloid Interface Sci.* **1999**, *220*, 302.
[2] H. Abe, Y. Hara, S. Maeda, S. Hashimoto, *J. Phys. Chem. B* **2014**, *118*, 2518.
[3] J. Ahmed, T. Yamamoto, H. Guo, T. Kurokawa, T. Nonoyama, T. Nakajima, J. P. Gong, *Macromolecules* **2015**, *48*, 5394−5401.
[4] C. K. Roy, H. L. Guo, T. L. Sun, A. Bin Ihsan, T. Kurokawa, M. Takahata, T. Nonoyama, T. Nakajima, J. P. Gong, *Adv. Mater.* **2015**, *27*, 7344.
[5] F. Luo, T. L. Sun, T. Nakajima, T. Kurokawa, Y. Zhao, A. Bin Ihsan, H. L. Guo, X. F. Li, J. P. Gong, *Macromolecules* **2014**, *47*, 6037.